The Carbohydrate Moieties of the β-Subunit of Na^+,K^+-ATPase: Their Lateral Motions and Proximity to the Cardiac Glycoside Site

Evzen Amler,* Alan Abbott,* Henryk Malak,‡ Joseph Lakowicz,‡ and William J. Ball, Jr.*
*Department of Pharmacology and Cell Biophysics, University of Cincinnati, College of Medicine, Cincinnati, Ohio 45267-0575, and ‡Center for Fluorescence Spectroscopy, Department of Biological Chemistry, University of Maryland, School of Medicine, Baltimore, Maryland 21201 USA

ABSTRACT The β-subunit associated with the catalytic (α) subunit of the mammalian Na^+,K^+-ATPase is a transmembrane glycoprotein with three extracellularly located N-glycosylation sites. Although β appears to be essential for a functional enzyme, the role of β and its sugars remains unknown. In these studies, steady-state and dynamic fluorescence measurements of the fluorophore lucifer yellow (LY) covalently linked to the carbohydrate chains of β have demonstrated that the bound probes are highly solvent exposed but restricted in their diffusional motions. Furthermore, the probes' environments on β were not altered by Na^+ or K^+ or ouabain-induced enzyme conformational changes, but both divalent cation and oligomycin addition evoked modest changes in LY fluorescence. Frequency domain measurements reflecting the Förster fluorescence energy transfer (FET) occurring between anthroylouabain (AO) bound to the cardiac glycoside receptor site on α and the carbohydrate-linked LY demonstrated their close proximity (18 Å). Additional FET determinations made between LY as donor and erythrosin-5-isothiocyanate, covalently bound at the enzyme's putative ATP binding site domain, indicated that a distance of about 85 Å separates these two regions and that this distance is reduced upon divalent cation binding and increased upon the $Na^+E_1 \rightarrow K^+E_2$ conformational transition. These data suggest a model for the localization of the terminal moieties of the oligosaccharides that places them, on average, about 18 Å from the AO binding site and this distance or less from the extracellular membrane surface.

INTRODUCTION

Na^+,K^+-ATPase is a plasma membrane protein whose primary physiological function is to maintain the Na^+ and K^+ cation gradients across cellular membranes. Therefore it plays a central role in maintaining the resting cell's membrane potential, in facilitating the transport of various ions and cellular metabolites, and as a receptor for cardiac glycosides (Jorgensen, 1986). Despite considerable study, the molecular mechanism of this pump and how it is regulated is still not fully understood. It is known to be composed of at least two subunits, the catalytic (α) subunit (M_r = 112 kDa) and the smaller glycoprotein (β) subunit ($M_r \approx$ 55 kDa, including its oligosaccharides). There may also be an associated low-molecular-weight polypeptide (γ) component (M_r = 7.7 kDa) (Collins and Leszyk, 1987). All of the known functional aspects of the enzyme are currently attributed to α. These include the Na^+, K^+, Mg^{2+} ATP, cardiac glycoside binding, and the ATP hydrolysis and P_i phosphorylation sites. In contrast to what is known about α the functional role of the β subunit is still largely unknown. Although there is no evidence that it binds any of the physiological regulators of enzyme activity, there is mounting evidence that its presence is essential for enzyme activity. Recent results show that α-mRNA alone is unable to direct the formation of active enzyme in either the *Xenopus* oocyte or yeast expression system (Horowitz et al., 1990; Noguchi et al., 1987). They also suggest that the extracellular portion of β may be important in determining the enzyme's affinity and response to both K^+ and Na^+ at the extracellular cation site (Eakle et al., 1992, 1995; Jaisser et al., 1992; Lutsenko and Kaplan, 1993).

Additionally, although β's participation in the reaction process remains uncertain, it appears to be required to ensure the correct folding of the α-subunit and the correct insertion, positioning, and transport of α to the plasma membrane. It may also protect newly synthesized α from proteolytic digestion (see review Chow and Forte, 1995). Consistent with at least some of these hypotheses is the observation by Tamkun and Fambrough (1986) that the assembly of αβ occurs concurrently with or immediately after polypeptide synthesis. In addition, Geering et al. (1989) have shown that the association of α with β renders α trypsin resistant, and that the coordinate synthesis of α and β is a prerequisite for the enzyme to leave the endoplasmic reticulum (Geering, 1991).

In terms of its structure and organization, β is asymmetrically oriented in the membrane with a short NH_2-terminal region on the intracellular side followed by one transmembrane section with the rest of the protein on the extracellular side of the membrane. The mammalian enzyme β-subunit

Received for publication 28 April 1994 and in final form 2 October 1995.

Address reprint requests to Dr. William J. Ball, Jr., Department of Pharmacology and Cell Biophysiology, University of Cincinnati College of Medicine, P.O. Box 670575, 231 Bethesda Ave., Cincinnati, OH 45267-0575. Tel.: 513-558-2388; Fax: 513-558-1169; E-mail: ballwj@ucbeh.san.uc.edu.

Dr. Amler was on leave from the Institute of Physiology, Czech Academy of Sciences, Prague, Czech Republic.

The present address of Dr. Abbott is Department of Chemistry, Louisiana State University, Shreveport, LA 71115.

The first two authors contributed equally to the work presented.

© 1996 by the Biophysical Society

0006-3495/96/01/182/12 $2.00

has three glycosylation sites (Shull et al., 1986; Brown et al., 1987), whereas fish and some amphibia (Zamofing et al., 1988) have four N-glycosylation consensus sequences. Although it seems likely that the sugar moieties have an influence on the enzyme's function, this has not been demonstrated. For example, the enzymatic removal of a majority of the sugars seems to have little effect on enzyme activity or ouabain binding (Sun and Ball, 1994). β does have three disulfide cysteine bonds that are extracellularly located and that should have an essential role in ordering the protein's structure (Kirley, 1989). They may be functionally important, inasmuch as it has been reported that mercaptoethanol-dependent reduction (with heating) of one or more of these disulfides results in the inactivation of the enzyme (Kawamura and Nagano, 1984; Ohta et al., 1986). Additional studies indicate that this inactivation, which is probably prompted by the partial reduction of all three cysteines rather than a single disulfide (Kirley, 1990), results from alterations of both extracellular and intracellular domains of α (Arystarkhova et al., 1995; Sun and Ball, 1994). Clearly, the molecular organization and interactions between the two subunits are important, even if they are not understood.

In this study we have used several fluorescent probes bound to the enzyme to obtain additional information about the structural and dynamic properties of the oligosaccharides of β and αβ interactions. We have used the procedures of Lee and Fortes (1985) to label the carbohydrates with the fluorophore lucifer yellow (LY). We have analyzed the steady-state and dynamic fluorescence properties of bound LY to deduce the probe's environment and motional properties. The spatial relationship between the α and β subunits was then investigated by Förster energy transfer (FET) measurements, with 9-anthroylouabain (AO) and LY as the donor/acceptor pair. The range of distances between these probes and the diffusional properties of the oligosaccharides were determined. In addition, the relatively large Förster distance (R_o) for the LY and erythrosin-5′isothiocyanate (ErITC) donor/acceptor pair made it possible to measure the approximate distance between the sugars on the extracellular side of the membrane and the ATP binding domain on the intracellular side and to determine ligand-induced changes in this distance.

MATERIALS AND METHODS

Na^+,K^+-ATPase isolation and characterization

The Na^+,K^+-ATPase was purified from the outer medulla of frozen lamb kidney according to the method of Lane et al. (1979). The initial activity of the enzyme was ~1100 μmol ATP hydrolyzed/mg protein/h as assayed spectrophotometrically according to the method of Schwartz (1969). The protein concentration was determined by the Lowry procedure, using BSA as the standard (Lowry et al., 1951).

Fluorescent probe labeling of Na^+,K^+-ATPase

The enzyme (1 mg/ml, 100 mM Tris, pH 9.1) was labeled with 10 μM ErITC, diluted from a 1 mM stock solution freshly dissolved in dimethyl sulfoxide, for 30 min in the dark at 23°C. The final concentration of dimethyl sulfoxide was 0.2% (v/v). The unreacted ErITC was separated from the labeled enzyme by centrifugation (100 × g) of the sample twice through a G-50 Sephadex column with a volume 3–5 times greater than the sample volume.

The enzyme was labeled with LY essentially as described by Lee and Fortes (1985). Briefly, 1 ml of the enzyme (4 mg/ml) was incubated with galactose oxidase (120 units), neuraminidase (2.8 units), and catalase (4000 units) in 50 mM Tris-HCl, 1 mM EGTA, pH 7.4, for 2 h at 0°C. This reaction was stopped by the addition of 5 mM dithiothreitol. The pH of the solution was then adjusted to 6.3 (using 1 M (2-[*N*-morpholino]ethanesulfonic acid, pH 5.9), and LY was added and incubated with the enzyme for 24 h at 0°C. The pH was then increased to 7.4 (Tris, pH 9.0), 25 mM $NaBH_4$ was added, and the incubation was continued for 30 min. The LY-labeled enzyme was then thoroughly washed by centrifugation and resuspension in 50 mM Tris-HCl, 1 mM EGTA, pH 7.4. Sodium dodecyl sulfate-polyacrylamide gel electrophoresis (SDS-PAGE) (Laemmli, 1970) of enzyme samples was performed with a BioRad minigel apparatus. The specificity of the LY labeling of β was demonstrated by using a transilluminator UV (365 nm) light box to monitor the fluorescent regions in the gels with the resolved protein bands, which were visualized by Coomassie brilliant blue staining. Fluorophore quantitation was done either spectrophotometrically or fluorometrically as appropriate, using known concentrations of free fluorophore to calibrate unknown fluorophore samples. For the fluorometric quantitations the fluorescence intensity of protein-coupled LY and ErITC was multiplied by the factors 1.1 and 0.256, respectively, to account for their changed fluorescence quantum yield upon reaction with the enzyme (see Results and Amler et al., 1992).

Steady-state fluorescence and absorbance measurements

All steady-state fluorescence data were obtained with an SLM/Aminco SPF-500 spectrofluorometer, and absorbance measurements with a UVIKON spectrophotometer. Samples were monitored at 25°C. Polarization data were obtained by exciting the samples with vertically polarized light, and the emission was observed through a polarized filter oriented first in the vertical (I_v) and then the horizontal (I_h) position. The total fluorescence intensity was calculated as $I = I_v + 2I_h$ and the anisotropy (r) value as

$$r = [(I_v/I_h) - G]/[(I_v/I_h) + 2G], \quad (1)$$

where G is the instrumentation factor that corrects the r value for the unequal detection by the fluorometer of vertically and horizontally polarized light.

AO binding and quantitation

Both LY-labeled and unlabeled enzyme was incubated with AO for 20 min at 37°C in 50 mM piperazine-*N*,*N*′-bis(ethenesulfonic acid), 5 mM Tris-P_i, 5 mM $MgCl_2$, pH 7.4. The fluorescence intensity increase that occurred upon AO binding to the enzyme was used to determine both the number of binding sites per milligram of protein and the affinity as outlined by Fortes (1986). The excitation wavelength used for AO was λ_{ex} = 367 nm with the emission wavelength, λ_{em} = 480 nm. The quantum yield of bound AO was ϕ = 0.27, and its extinction coefficient ϵ = 7800 M^{-1} cm^{-1} at 362 nm.

Analysis of collisional quenching data

Iodine (choline iodide, or KI) and cesium (CsCl) salts were added as fluorescence quenchers over the 0–50 mM and 0–500 mM concentration ranges, respectively, to solutions of the LY-labeled enzyme, and the resultant decreases in LY fluorescence intensity were determined (λ_{ex} = 428, λ_{em} = 540 with ϵ = 11,900 cm^{-1} and ϕ = 0.21 in water; Stewart, 1978). All titrations were performed in triplicate, and the quenching

constants or K_D values were derived from the linear slopes of the Stern-Volmer (F_o/F versus [Q]) plots using the equation

$$F_0/F = 1 + K_D[Q], \quad (2)$$

where F_o and F are the fluorescence intensities of the fluorophore in the presence and absence of the quencher and [Q] is the molar concentration of quencher. The bimolecular collisional rate constant, k_q, was found by dividing the Stern-Volmer constant (K_D) by the probe's unquenched fluorescence lifetime (τ_o) and is a lifetime-independent measurement of solvent accessibility.

Dynamic fluorescence measurements

Frequency-domain measurements were performed to determine the fluorescence decay lifetimes of the free and enzyme-bound fluorophores using the instrumentation previously described by Lakowicz et al. (1986) and Laczko et al. (1990). AO was excited at 367 nm by frequency doubling of the excited emission from a pulsed dye laser (pyridine 1, as the dye) driven by an Argon ion-mode locked laser (λ_{em} = 514 nm). Phase and modulation measurements were made over 15–2000 MHz. LY was excited at 442 nm by a He-Cd (cw) laser with a Pockel cell as light modulator over the 10–150 MHz frequency range. The fluorescence emissions from AO and LY were observed through Corning cut-off filters 3-73 (λ = 430 nm) and 3-70 (λ = 500 nm), respectively. Magic angle polarizer conditions were used for dynamic fluorescence measurements. The temperature of the samples was held at 25°C by a circulating water bath. An aqueous suspension of LUDOX was used as a reference sample. Corrections for background protein fluorescence or light scattering were made by performing frequency-domain measurements using unlabeled enzyme as the control and then correcting the data in the manner described by Lakowicz et al. (1987a). The experimental data were collected using a DEC PDP 11/23 computer and then transferred to a DEC PDP 11/73 system for analysis in terms of a sum of exponentials as described previously (Lakowicz et al., 1984), using a nonlinear least-squares routine for multiexponential fitting and additional software available at the Center for Fluorescence Spectroscopy (University of Maryland, Baltimore). The χ^2 parameter was used to judge the quality of the fit of the phase (ϕ) and modulation (m) data:

$$\chi^2_R = \frac{1}{N}\sum_{\omega}\frac{(\phi_\omega - \phi_{c\omega})^2}{\sigma_\phi} + \frac{1}{N}\sum_{\omega}\frac{(m_\omega - m_{c\omega})^2}{\sigma_m}. \quad (3)$$

Here N is the number of degrees of freedom, and σ_ϕ and σ_m are the experimental uncertainties in the measured phase (ϕ_ω) and modulation (m_ω) values. ϕ_{cw} and $m_{c\omega}$ are the calculated phase and modulation values, respectively. For all analysis the uncertainties in the phase and the modulation were taken as 0.2 and 0.005, respectively. The lifetime distribution analysis was derived from the measured data according to the method of Fiorini et al. (1987) and used a Lorentzian probability distribution fit of (τ_i):

$$\alpha(\tau) = \sum_i \frac{1}{\pi}\frac{(\text{FWHM})/2}{(\tau_i - \tau)^2 + (\text{FWHM}/2)^2}, \quad (4)$$

where τ is the center of the lifetime distribution, FWHM is the full width of the distribution at the half-maximum, and α is a normalization constant.

Förster energy transfer measurements and calculations

Steady-state determinations of acceptor-dependent quenching of donor fluorescence occurring with the AO/LY pair were made spectrofluorometrically with λ_{ex} = 364 nm, λ_{em} = 460 nm and for the LY/ErITC pair with λ_{ex} = 428 nm, λ_{em} = 540 nm and bandpass widths for excitation and emission set at 4 and 10 nm, respectively. For the dynamic measurements with the AO/LY pair upon laser light excitation at 367 nm the AO fluorescence was selectively observed using an interference filter with λ = 430 nm, bandpass width = 12 nm.

The apparent efficiency (E) of Förster energy transfer (FET) was determined from the extent of acceptor-dependent quenching of the donor fluorophore's steady-state fluorescence intensity, where F and F_o are donor fluorescence intensities in the presence or absence of acceptor or calculated from the fluorescence decay lifetimes (τ), and preexponential factors (α) are obtained by frequency domain analysis (in the presence and absence of acceptor) with

$$\frac{F}{F_o} = (\sum_i \alpha_i\tau_i)/(\sum_i \alpha_i\tau_i)_o = 1 - E. \quad (5)$$

The distance (R) separating the donor/acceptor pair was calculated from the efficiency of Förster energy transfer using the equation

$$R = R_o[(1 - E)/E]^{1/6}, \quad (6)$$

where R_o is the Förster radius, or the distance at which there is 50% energy transfer and which is calculated from

$$R_o^6 = \left[\frac{9000(\ln 10)\,K^2\phi D}{128\pi^4 N n^4}\right]\int_0^\infty F_D(\lambda)\varepsilon_A(\lambda)\,\lambda^4\,d\lambda, \quad (7)$$

where K^2 is the orientation factor, ϕ the quantum yield of the donor D in the absence of acceptor A, n is the refractive index of the solution, N is Avogadro's number, $F_D(\lambda)$ is the corrected fluorescence intensity of the donor in the wavelength range λ to $\lambda + d\lambda$, with the total fluorescence intensity normalized to unity, and ϵ_A is the extinction coefficient of the acceptor. The values of ϕ_D and ϵ_A at λ_{max} (428 nm), for bound LY are ϕ_D = 0.21, and ϵ_A = 11,900 $cm^{-1}M^{-1}$. The ϕ_D for bound AO (only used as donor) = 0.27, whereas for bound ErITC (only used as acceptor) ϵ_A = 88,000 $cm^{-1}M^{-1}$ at λ_{max} = 535 nm.

The donor/acceptor distances between AO and LY were also analyzed assuming a static Gaussian probability distance distribution:

$$P(r) = \frac{R}{\sigma\sqrt{2\pi}}\exp\left[\frac{1}{2}\frac{(R - R_o)^2}{\sigma}\right], \quad (8)$$

where r is the average and σ is the standard deviation of the distribution which is related to the full-width at half maximum (FWHM), with FWHM = 2.354 σ. The distance distribution was derived from the heterogeneity of the frequency response of the donor (AO) in the presence of acceptor LY, and the data were analyzed assuming a multimodal distance distribution between probes (expressed by the observed multiexponential donor decay) according to the model of Lakowicz et al. (1988). The analysis of the donor/acceptor distance distribution, including the diffusional change in distance, was performed using the software developed at the Center for Fluorescence Spectroscopy at the University of Maryland School of Medicine (see Lakowicz et al., 1990).

Materials

The buffers and chemical reagents as well as the ErITC and LY were obtained from Sigma Chemical Co., and AO was obtained from Molecular Probes (Eugene, OR). The N-glycanase F was purchased from Genzyme Corporation.

RESULTS

Labeling of the Na^+,K^+-ATPase by LY

The enzyme was labeled over a range of LY concentrations (0.5–5 mM) as described in Materials and Methods. Polyacrylamide gel electrophoresis of the enzyme was then

employed to confirm the specificity of the labeling on the β subunit. Monitoring the LY fluorescence of the resolved subunits showed that essentially all labeling occurred on β. The activity of the enzyme was decreased 6% by the labeling procedure, but the actual reaction with LY had no additional effect on enzyme activity (see Table 1). Furthermore, the extent of LY labeling also increased as higher concentrations of LY were used, with a ratio of about 1.5 nmol LY/nmol of enzyme when 5 mM LY was used (Table 1). These results were in good agreement with the previous work done with the dog kidney Na^+,K^+-ATPase by Lee and Fortes (1985).

Determination of the environment of enzyme-bound LY

Upon covalent binding to the enzyme's carbohydrates the absorption and fluorescence emission spectra of LY were essentially unchanged from that of the free probe (data not shown). This suggested that the bound probe remained largely exposed to the polar, aqueous environment of the solution buffer. This was further confirmed in that enzyme-bound LY also did not dramatically change its average lifetime of fluorescence decay. Frequency-domain fluorometry showed that the fluorescence of the free probe decayed as a single exponential with a lifetime of $\tau = 5.06$ ns. For the enzyme-bound probe the decay curve clearly became more complex, because a two-lifetime component model (2.5 and 5.8 ns) was required to fit the data, but the average decay lifetime remained essentially unchanged (Table 2). Furthermore, the steady-state fluorescence intensity of LY decreased ~10% upon reaction with the enzyme. This became apparent when the fluorescence intensity of Na^+,K^+-ATPase-bound LY was found to increase about 10% without any change in its absorption spectrum when the enzyme was denatured in 0.2% SDS, whereas the free probe showed no response to SDS. This suggested that about 10% of the LY fluorescence was statically quenched upon linkage to the polysaccharides. All fluorescence intensity comparisons of bound and free LY have, therefore, been corrected for this quenching.

TABLE 1 Lucifer yellow labeling on Na,K-ATPase activity

LY conc. (mM)	0	0.5	2	5
Enzyme activity (% of maximum)	94 ± 6	92 ± 8	99 ± 9	93 ± 9
Fluorescence (a.u.)	0	100 ± 2	119 ± 7	137 ± 6
Anisotropy	N/A	0.176 ± .003	0.165 ± .003	0.153 ± .004
Stoichiometry	0	1.07	1.27	1.5

Na^+,K^+-ATPase was labeled with 0–5 mM lucifer yellow (LY) as described in Materials and Methods. Na^+,K^+-ATPase activity was measured in triplicate. The relative activity and standard deviations were calculated from triplicates as a percentage of the activity of untreated enzyme. The steady-state fluorescence intensity of 5–10 μg/ml LY-labeled enzyme, given in relative arbitrary units (a.u.), and anisotropy values were also measured in triplicate with the excitation wavelength, 428 nm and emission wavelength, 535 nm. The number of fluorophores (LY) per β-subunit was calculated from steady-state fluorescence intensity of washed, labeled Na^+,K^+-ATPase assuming 10% fluorescence quenching of LY after binding (see text) and the molecular weight of Na^+,K^+-ATPase = 150,000.

TABLE 2 Analysis of lucifer yellow intensity decay

Sample	α_i	τ_i(ns)	$\langle\tau\rangle$(ns)	χ^2_R
LY (free label)	1.000	5.06	5.06	1.9
LY-Na,K-ATPase	1.000	4.48	4.48	60
τ_1	0.418	2.5		
τ_2	0.582	5.8	5.01	2.4
LY-Na,K-ATPase +5 mM MgCl2	1.000	4.77	4.77	24
τ_1	0.965	4.44		
τ_2	0.035	15.5	5.68	2.8

LY fluorescence intensity decays were fit to one- and two-component models. The free label (10 μM in 50 mM Tris-HCl, 1 mM EDTA, pH 7.4 buffer) decayed as one component, whereas the bound fluorophore (100 μg/ml LY-enzyme, in buffer) decayed as two as judged by the reduced χ^2_R. The lifetime components (τ_i) and in preexponential factors (τ_i) were used to calculate the mean lifetime, $\Sigma\alpha_i\,\tau_i^2/\Sigma\alpha_i\,\tau_i$.

In terms of the rotational freedom of the bound probe, the anisotropy ($r = 0.176$, Table 1) value was found to be significantly higher than that of free probe ($r = 0.01$) but lower than that for complete immobilization ($r = 0.33$, calculated from anisotropy decay data). In addition, the anisotropy of bound LY decreased substantially upon SDS addition ($r = 0.09$). These data suggest that the native protein structure limits the rotational motion of the probe. As shown in Table 1, the anisotropy value also decreased somewhat as the number of enzyme-linked LY molecules increased, which suggested that there is some heterogeneity among the labeled sites.

The effects of cations upon LY fluorescence properties

Although the cation-dependent transition between the $Na^+E_1 \rightarrow K^+E_2$ conformational forms of the enzyme is known to occur with distinct structural changes, we found that the addition of Na^+ or K^+ ions did not alter the fluorescence intensity or anisotropy of carbohydrate-linked LY. The steady-state fluorescence intensity of bound LY was affected, however, by the addition of divalent cations. In the millimolar concentration range, magnesium ($\Delta F = -3\%$ and -5% at 1 and 5 mM, respectively), manganese, and calcium each were found to cause modest decreases in the LY-Na^+,K^+-ATPase fluorescence. There decreases were very similar to that reported previously by Lee and Fortes (1986). When the lifetime(s) of LY were further analyzed by frequency-domain fluorometry (over the modulation frequency range of 7–125 MHz), either as distributions or as discrete values, they were found to be altered by 5 mM Mg^{2+}. As shown in Fig. 1, upon Mg^{2+} addition, the two lifetime components of enzyme-bound LY essentially shifted to a single value (with a small fraction of a very long-lived component) distinct from either of the lifetimes

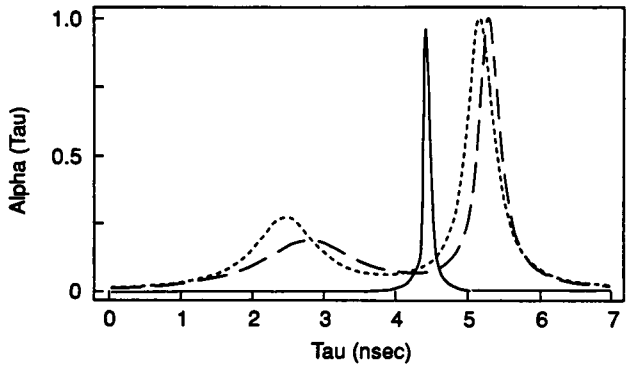

FIGURE 1 Fluorescence lifetime distribution of LY-Na^+,K^+-ATPase. The Lorentzian lifetime distribution of LY-Na^+,K^+-ATPase (100 μg/ml) fluorescence was observed in the absence (···) and in the presence (——) of 5 mM $MgCl_2$, and upon addition of oligomycin to the Mg^{2+}-containing sample (– – –). The distributions were normalized to 1.0.

obtained in the absence of ligands (Table 2). These effects, occurring at cation levels above those required for Mg^{2+} regulation of enzyme activity but approximating the combined extracellular concentrations of Mg^{2+} and Ca^{2+}, may result from direct interaction with the LY-labeled oligosaccharides.

Determination of the solvent accessibility of LY

The accessibility of the bound LY to positive and negative collisional quenchers was determined by using KI and CsCl as quenching ions. The data in Table 3 show that the negative quencher (I^-) gave a bimolecular quenching constant (derived in Materials and Methods) k_q = 2.35 nM^{-1} s^{-1} for LY in solution, and this value decreased about 60% (k_q = 0.94 nM^{-1} s^{-1}) upon its covalent coupling to the carbohydrates of β. In contrast, the positively charged quencher Cs^+, which was a much less effective quencher of LY than I^-, gave a higher k_q value for bound LY than for free probe. This suggested that there may be charge-charge interactions occurring in the region of the bound LY, with the negatively charged quencher (I^-) encountering some negative charge repulsion while the access for Cs^+ was enhanced. The addition of Mg^{2+} caused a small but reproducible decrease in the quenching constant of both quenchers.

TABLE 3 Determination of I^- and Cs^+ quenching constants for LY

	Bimolecular quenching constants k_q (M^{-1} s^{-1} × 10^{-9})			
	KI		CsCl	
Quencher	(−)Mg^{2+}	(+)Mg^{2+}	(−)Mg^{2+}	(+)Mg^{2+}
Lucifer yellow	2.35 ± 0.08	2.35 ± 0.08	0 ± .0.1	0
Lucifer yellow-Na^+,K^+-ATPase	0.94 ± 0.04	0.83 ± 0.04	0.07 ± 0.01	0.067 ± 0.01

The fluorescence of LY-Na^+,K^+-ATPase (5 μg/ml, in 50 mM Tris-HCl, 1 mM EDTA, pH 7.4) was quenched with increasing concentrations of KI or CsCl in the absence or presence of 5 mM $MgCl_2$. The resultant curves were analyzed by the Stern-Volmer equation ($F_o/F = 1 + k_q \tau_o$ [Q]) and gave linear plots. The bimolecular constants were calculated as described in Materials and Methods.

Ouabain and oligomycin interactions with LY

Ouabain and oligomycin are both inhibitors of Na^+ pump activity, whose binding is localized to the extracellular side of the membrane (Cornelius and Skou, 1985), but their inhibitory mechanisms are distinct. Ouabain, with the appropriate ligands present, stabilizes an $E_2 - P_i$·ouabain conformation. Oligomycin, in contrast, enhances Na^+ affinity and stabilizes an occluded (Na^+)E_1 conformation of the enzyme. For ouabain binding conducted under Mg^{2+} and $Mg^{2+}P_i$ conditions, no effects upon LY fluorescence were observed. Oligomycin, though, increased LY fluorescence and its anisotropy value (Table 4). In this work an oligomycin concentration of 10 μg/ml (approximately 13 μM) was used because it inhibited the enzyme's ATPase activity by about 73% without excessive light scattering. Upon addition of oligomycin to the enzyme an initial increase in light scattering occurred in a matter of minutes, which then decreased slowly over a period of 30 min with no change of the steady-state LY fluorescence spectrum. The residual light scattering as measured with oligomycin and unlabeled enzyme as a background control was less than 5% of the LY fluorescence signal and was substracted. Table 4 shows that oligomycin binding caused increases in both the fluorescence intensity of LY and the anisotropy (r) value. These results suggest that oligomycin binding, unlike ouabain, exerts an effect on β as well as α.

In addition we found that the binding site of the cardiac glycosides appears physically distinct from that (those) of oligomycin, because oligomycin did not alter the final level of anthroylouabain (AO) binding (a fluorescent ouabain derivative) nor the quantum yield increase that occurred upon its binding. Oligomycin, however, reduced the rates of ligand-induced E_1 to E_2 transitions but not $E_2 \rightarrow E_2$-P_i transitions. The K^+-dependent (10 mM) $Na^+E_1 \rightarrow$ (4 mM) K^+E_2 and ouabain-dependent $Mg^{2+}E_1 \rightarrow Mg^{2+}E_2$·ouabain rates of transitions, as monitored by the fluorescent changes in fluorescein (FITC)-labeled enzyme (Abbott et al., 1991),

TABLE 4 Effect of oligomycin on LY steady-state fluorescence intensity and anisotropy

Sample	Fluorescence (a.u.)	anisotropy
LY-Na^+,K^+-ATPase		
+ oligomycin	2.9	0.167
	3.6	0.207

The fluorescence intensity (a.u.) and anisotropy of lucifer yellow-labeled Na^+,K^+-ATPase (LY-Na^+,K^+-ATPase, 5 μg/ml) was measured in 0.05 M Tris, 10 mM NaCl, and 10 mM $MgCl_2$, pH 7.4, at 37°C before and after incubation for 1 h in 10 μg/ml oligomycin. Contributions of background light scattering (see text) were subtracted using an unlabeled enzyme control.

were decreased approximately three- and tenfold, respectively. Essentially no inhibition by oligomycin was observed for the (K^+) $Mg^{2+}E_2$, ouabain plus $P_i \rightarrow (K^+)$ $Mg^{2+}E_2$-P_i·ouabain transition. These ouabain and oligomycin interactions appear consistent with those reported by Taniguchi et al. (1991) using the *N*-(*p*-(2-benzimidlazolyl)-phenyl)maleimide fluorescent probe-labeled enzyme.

Determination of the distance(s) between the LY-labeled β-carbohydrates and the cardiac glycoside binding site on α

To better understand the relative locations of and potential interaction between the extracellularly located carbohydrates on β and the cardiac glycoside binding site on α, the distance between the fluorescent cardiac glycoside derivative anthroylouabain (AO) and LY was measured by Förster energy transfer (FET). The emission spectrum of AO (λ_{max} = 480 nm) completely overlaps the absorption spectrum of LY λ_{max} 428 nm; thus AO can serve as donor and LY as acceptor. To observe steady-state FET between these probes identical concentrations (100 μg/ml) of LY-labeled and unlabeled Na^+,K^+-ATPase were titrated with AO. High levels of enzyme (tenfold the K_d value of AO) were used so that initially complete binding of AO was observed. Fig. 2 shows that both enzyme samples were saturated at ~0.28 μM AO and therefore displayed the same number of AO binding sites. The initial slope of the fluorescence intensity versus AO concentration curve was, however, 39% lower for AO binding to the LY-enzyme as compared to the unlabeled enzyme. Furthermore, unlabeled enzyme subjected to the labeling procedures (the galactose oxidase, neuraminidase, and $NaBH_4$) but without LY gave the same results as untreated enzyme. The reduced fluorescence intensity of AO induced by the presence of LY on β clearly indicated the occurrence of nonradiative energy transfer.

At AO concentrations above 0.30 μM the slopes of the fluorescence plots decreased, and as expected for free or nonspecifically bound AO, they were identical for both samples. To calculate the distance(s) between probes the R_o critical or the calculated distance for 50% transfer efficiency was determined to be R_o = 30 Å (see Materials and Methods). In this specific case, however, the number of LY molecules bound per β-subunit (2 mM LY was used for labeling) was greater than the number of AO binding sites (1.4 mol/mol), and the calculated R_o was modified to correct for multiple energy transfer events. To do this we assumed that LY acceptors were at an average distance *R* from a donor. The apparent rate of energy transfer (k_t app) is then the true rate times the ratio of acceptors to donors:

$$k_{t\,app.} = 1.4\,k_t. \tag{9}$$

The rate constant k_t varies as the sixth power of *R*:

$$k_t = (1/\tau_o)(R_o/R)^6, \tag{10}$$

where τ_o is the initial lifetime of the excited state of the donor. The corrected R_o is then

$$R_{o\,corr} = \sqrt[6]{1.4}\,R_o, \tag{11}$$

and represents only a 5% increase. The fluorescence energy transfer efficiency was therefore calculated from the data shown in Fig. 2 (E = 39%), giving a calculated average distance between the LY molecules and AO of r = 34 Å, which is 13 Å shorter than the value (47 Å) reported by Lee and Fortes (1986). It is clear, though, with three different oligosaccharide chains on β and perhaps up to 12 different sites for LY linkage (Treuheit et al., 1993), that the LY is likely to be distributed over a range of sites and distances from the donor.

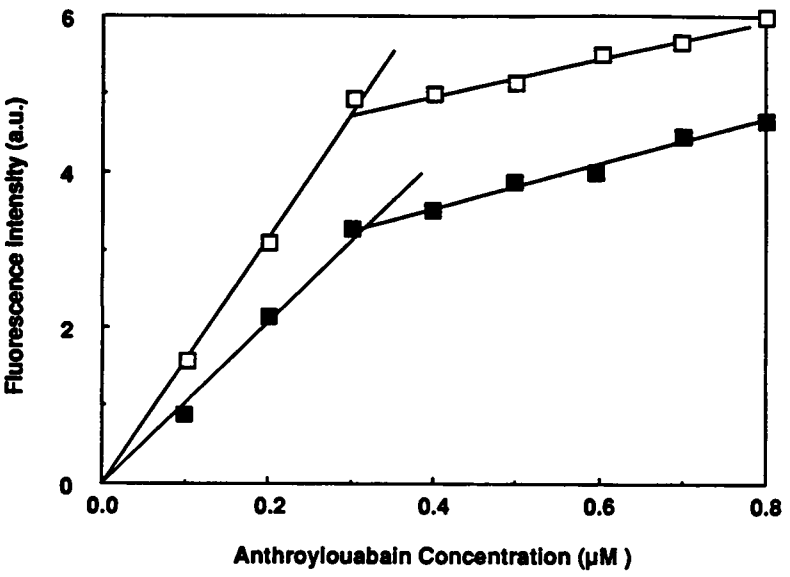

FIGURE 2 Titration of Na^+,K^+-ATPase and LY-labeled Na^+,K^+-ATPase with AO. Untreated Na,K-ATPase (100 μg/ml; □) and LY-Na,K-ATPase (100 μg/ml; ■) were titrated with increasing concentrations of AO and the fluorescence of AO (λex = 364 nm; λem = 460 nm) monitored. The reduced (39%) slope of the fluorescence versus μM AO concentration for the LY-labeled enzyme results from a reduction in the quantum yield of bound AO due to AO/LY energy transfer.

TABLE 5 Determination of the excited state lifetimes of anthroylouabain

Sample	Component	α_i	τ_i (ns)	I (%)	$\langle\tau\rangle$ (ns)	X_R^2
AO	τ_1	0.961	0.60	85	0.90	7.3
	τ_2	0.039	2.55	15		
AO-Na,K-ATPase	τ_1	0.55	1.0	15		
	τ_2	0.45	6.7	85	5.8	2.0
AO-LY-Na,K-ATPase	τ_1	0.68	0.3	17		
	τ_2	0.23	1.4	29		
	τ_3	0.09	6.5	54	3.9	2.5
AO-LY-Na,K-ATPase + oligomycin	τ_1	0.87	0.1	12		
	τ_2	0.10	1.3	36		
	τ_3	0.03	6.9	52	4.0	3.7

Na^+,K^+-ATPase (or LY-Na^+,K^+-ATPase, 0.74 mg/ml) was incubated with 5 μM AO in 50 mM PIPES, 5 mM Tris-P_i, 5 mM $MgCl_2$, pH 7.4, for 30 min at 37°C. Where indicated oligomycin (10 μg/ml final concentration) was incubated with AO-labeled LY-Na, K-ATPase for an additional 30 min at 37°C. The frequency response of AO fluorescence with excess enzyme was measured using frequency-domain methods (modulation frequencies 15–330 MHz) and analyzed as described in Materials and Methods. For each component, τ_i is the decay time, α_i the preexponential factor, and I (%) is the fractional intensity.

Lifetime and FET determinations from frequency-domain fluorometry

To assess the energy transfer distance heterogeneity that might result from having both highly quenched and unquenched populations of bound AO, frequency-domain lifetime distributions were determined for AO free in solution, bound to native enzyme, and bound to LY-labeled enzyme (Table 5). Lifetimes were calculated from the frequency response data obtained over the frequencies 15–339 MHz. These data were corrected for the background responses of enzyme alone as well that of the LY-labeled enzyme (Lakowicz et al., 1987a) under AO excitation and emission conditions. Treating the fluorescence decays as a sum of exponentials showed that a two-exponential decay model was sufficient to fit the data (τ_1 = 1.0, τ_2 = 6.7 ns) for enzyme-bound AO. A two-component decay was also observed for free AO in buffer (see Table 5), but the average lifetime was 6.5 times lower. Therefore, in an aqueous solution, a complex lifetime is intrinsic to this probe and is not just the result of its binding the receptor. The fluorescence decay of AO in the presence of the acceptor LY (1.4 mol/mol β) became more complex as well as faster and was best fit by a three-component model. Interestingly, the lifetime values showed that the predominant component (68%) had a short 0.3 ns value but about 9% of the bound AO had a lifetime that was essentially the same as the long-lived component observed in the absence of acceptor. This suggested that a portion of the β-subunits remained unlabeled by LY or some fraction of AO did not interact with LY. This uneffected population could cause an overestimate of the AO-to-LY distance.

The effect of this long lifetime component on the distance calculation was further considered by analyzing the lifetime data as a Gaussian probability distribution of distances between probes (Lakowicz et al., 1987b) rather than as a collection of discrete lifetimes. In our case a model generalized to include multiple lifetime donors and acceptors was used (Lakowicz et al., 1988). Unlike the steady-state measurements, in this analysis the AO lifetime component unchanged by the presence of the LY acceptor (where $R \gg R_o$) will occupy only a minor fraction of the distance distribution. This model fit the data (χ_R^2 = 2.5) as well as that obtained using the three-exponential fit (Table 5). In addition, it had only two floating parameters (r, the average distance and FWHM), whereas the discrete lifetime analysis contained five (three lifetime and two α_i, normalized preexponential factors) parameters. Fig. 3 shows that the average derived distance r between AO and LY was 17.8 Å, with a full-width range at half-maximum (FWHM) of 15.7 Å. The broadness of this distribution is clearly consistent

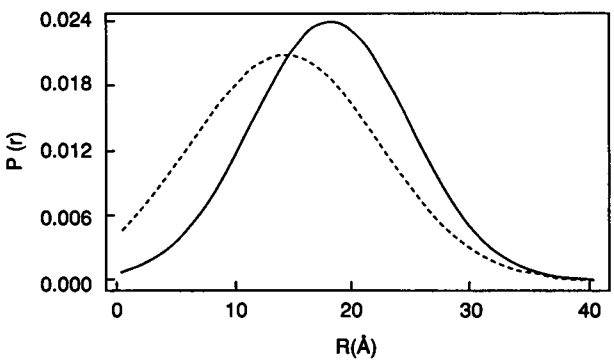

FIGURE 3 The distance distribution between bound AO and carbohydrate-linked LY on Na^+,K^+-ATPase (0.74 mg/ml). The distribution of distances between AO and LY in the absence (——) and in the presence (– – –) of oligomycin (10 μg/ml) are plotted. Förster energy transfer distances were calculated as a static Gaussian distribution from frequency-domain data as described by Lakowicz et al. (1987b). The mean distance was 17.9 Å and the FWHM 15.7 Å, respectively, without oligomycin and 14.1 Å, respectively, in the presence of oligomycin.

with LY labeling the oligosaccharides at more than one spatially distinct location (Lakowicz et al., 1988). In addition, this average distance was about 16 Å shorter than that estimated by the steady-state data. Next the effects of oligomycin on the AO lifetimes and AO/LY distance distribution were determined. This inhibitor only slightly altered the distribution of the lifetime components (Table 5), but this decreased the average distance another 4 Å while further broadening the distance distribution (Fig. 3). With no discernible alteration in the AO site, we infer that these modest oligomycin effects reflect an alteration at the β-carboyhydrates.

Analysis of the diffusional distribution or motion of LY

We also investigated the possibility of a dynamic distribution of energy transfer distances. In this model the distribution of AO/LY distances is caused by the diffusional motion of the LY-labeled carbohydrates during the lifetime of the energy transfer process. Therefore we analyzed the frequency-response data using a dynamic distribution model developed by Lakowicz et al. (1990). The resulting fit was no better than that obtained using the static model ($\chi^2_R = 2.7$), and it yielded the same value for the average distance between the probes (r = 17.8 Å) and a similar width of the distribution (FWHM = 15.7 Å). In addition, the derived diffusion constant (D) was $4 \pm 3 \times 10^{-9}$ cm^2/s, using this value in the Einstein relation ($\langle d \rangle^2 = 2D \cdot t$, assuming one dimension for diffusion), and the average root mean squared distance (d) diffused by the oligosaccharides during the average AO donor lifetime was calculated to be less than 1 Å. The large uncertainty in the D value is typical for these analyses, but d only increases 10% when D is increased by two standard deviations. Interestingly, this calculated d value for LY on the carbohydrates is approximately that obtained for the holoenzyme in fluorescence recovery after photobleaching (FRAP) experiments (Amler, unpublished results). Thus, the static model provided an adequate fit to the measured data, and this suggested that the oligosaccharides of β are diffusionally restricted.

Determination of the distance between the LY-labeled β-carbohydrates and the ATP binding site of α

The fact that the emission spectrum of LY also overlaps well with the absorption spectrum of ErITC (Fig. 4) also made this donor/acceptor pair (LY/ErITC) suitable for long-distance Förster energy transfer determinations. This measurement is of interest because ErITC is a fluorescent molecule that labels α at or near its ATP binding site, and we have previously measured its distance from the glycoside site (Amler et al., 1992). We calculated the overlap integral between LY and ErITC, taking into consideration the 10% lower fluorescence intensity of LY after reaction with the β-subunit carbohydrates and determined the characteristic Förster distance (R_o, Eq. 7) to be equal to 59.9 Å. Because the degree of rotational freedom for LY was reasonably high (r = 0.176), the orientation factor K^2 (Eq. 7) was assumed to be 2/3. Energy transfer was observed by monitoring the quenching of the fluorescence intensity of LY-Na^+,K^+-ATPase upon labeling the enzyme with ErITC.

The LY fluorescence was found to decrease by 8% in the presence of bound ErITC. But since, as with FITC, there is nonspecific labeling with the ErITC labeling of the enzyme,

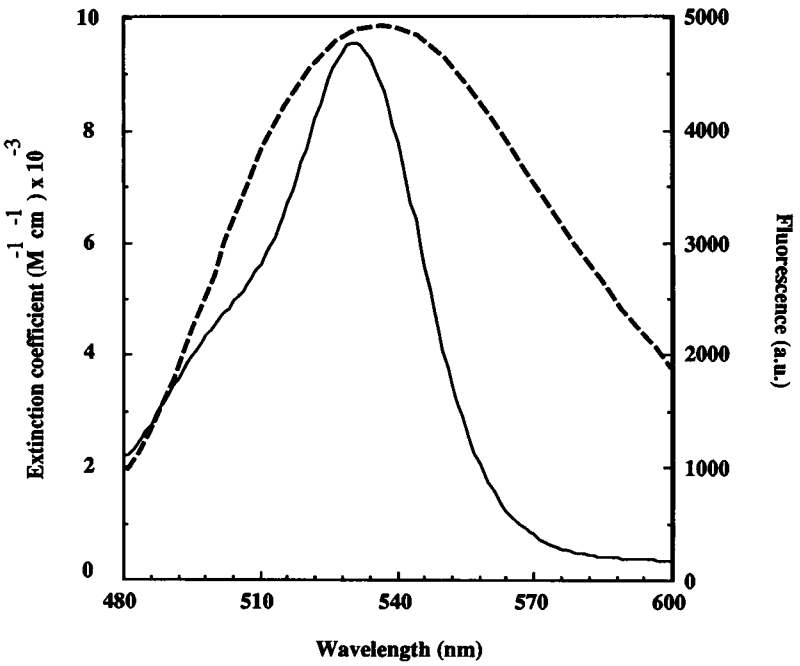

FIGURE 4 Determination of the overlap between the fluorescence emission spectrum of LY and the absorption spectrum of ErITC. The emission spectrum of lucifer yellow (– – –, excitation wavelength = 442 nm) strongly overlaps the absorption spectrum of ErITC (——). From the overlap integral the calculated Forster distance for donor/acceptor pair LY/ErITC as R_o = 59.9 Å (see Materials and Methods).

which is only partially blocked by the presence of ATP (Amler et al., 1992), we needed to account for the contribution of this unlocated population to any of the FET observed. When ErITC labeling was done in the presence of 10 mM ATP, so that the labeling was predominantly nonspecific, only a 3.0% quenching decrease in LY fluorescence occurred. In a simplified treatment of the results, the direct subtraction of this value from the initial 8% observed would give a specific FET value of 5.0%. This value would generate a calculated LY-to-ErITC distance of about 98 Å. To correctly interpret these data, though, we need to eliminate the contribution to FET from nonspecific ErITC and take into account the molar ratio of site-specific ErITC labeling and the stoichiometric excess (1.4 mole/mole β) of the donor (LY) labeling. The total level of ErITC labeling was spectrofluorometrically determined to be 0.99 mol ErITC/mol α-subunit. The number of ATP binding sites labeled was then assumed to be equal to the determined number of AO binding sites, 0.42 mol/mol α (see Fig. 3), thus leaving 0.57 mol per α of nonspecific ErITC labeling. This is only a slightly lower level of specific ErITC labeling than that obtained in our previous ATP protection studies (Amler et al., 1992).

The observed energy transfer efficiencies (E) can then be converted to uncorrected or virtual transfer rate constants (k_t), which allows us to correct for the incomplete labeling by ErITC and calculate E specific. The conversion is done using the equation (Lakowicz, 1983)

$$E = k_t \tau_o/(1 + k_t \tau_o). \quad (12)$$

The total uncorrected rate constant k^{unc} is the sum of the uncorrected specific (sp) k^{unc} and nonspecific (nsp) k^{unc} constants:

$$k_{tot}^{unc} = k_{sp}^{unc} + k_{nsp}^{unc} = E^{tot}/\tau_o\,(1 - E^{tot}), \quad (13)$$

where τ_o is the lifetime of the donor in the absence of acceptor. Consideration of the labeling stoichiometries of the donor (1.4 LY/α subunit) and the specific (0.42) and nonspecific labeling (0.57 mol/α) of the acceptor ErITC results in the true overall rate constants (k_{tot}):

$$k_{tot} = 1/1.4\,(k_{tot}^{unc}) = 0.42\,k_{sp} + 0.57\,k_{nsp}, \quad (14)$$

where k_{sp} and k_{nsp} are the true specific and nonspecific rate constants, respectively. The corrected specific rate constant (k_{sp}) is then

$$k_{sp} = 1/1.4\,k_{tot}^{unc} - 0.57\,k_{nsp}^{unc}\,(1/0.42). \quad (15)$$

Equation 12 was used to determine k_{tot}^{unc} and k_{sp}^{unc} with $E^{tot} = 0.08$ and $E_{nsp} = 0.03$, respectively. Then solving Eq. 15 gives the rate constant $k_{sp} = 0.024\ ns^{-1}$. Converting this rate constant to the specific transfer efficiency using Eq. 12 gives $E_{sp} = 0.107$, and the distance from LY to the ATP binding (or specific ErITC labeling) site was calculated to be 8.5 nm (85 Å). For an approximate error analysis, this distance was recalculated using different values of labeling stoichiometries and energy transfer efficiencies. A 1 Å change in the calculated distance occurred when the specific labeling stoichiometry (42%) was changed by ±5% and when the total FET efficiency value (8%) was changed by ±0.5% (a 6.2% relative change). A less than 0.5 Å change occurred with a similar ±5% alteration in the level of nonspecific labeling. Actual measurements of the stoichiometries varied by 5%, and FET efficiencies by 0.5%.

Thus although the calculated value of 85 Å is clearly only an approximation, given the relatively modest FET observed and the assumptions made in this complex system, this value appears reasonable and the actual distance is not likely to be significantly shorter than this or greater than the calculated simplest value of 97 Å.

In addition, the extent of FET observed was altered by some ligand conditions. Increasing concentrations of Na^+ (1 mM to 10 mM, in Tris buffer) had no effect on the LY (nor ErITC) fluorescence intensity, but a fluorescence increase, or a decrease in FET efficiency (from 8% to 7%), was observed upon the addition of 2 mM KCl. Because no FET change occurred for the LY-enzyme sample labeled nonspecifically with ErITC, this change in the site-specific FET efficiency could represent a 2–3 Å increase in the distance between the two probes upon the $Na^+E_1 \rightarrow K^+E_2$ enzyme conformation transition. Mg^{2+} was then found to increase in the FET from 8% to 10%. This change resulted in a calculated decrease in the LY-to-ErITC distance of approximately 4 Å. After Mg^{2+} addition, the K^+-induced effect was still observed and it was therefore an independent process. Interestingly, whereas here we report evidence for ligand-induced changes in the reported distances between the two sites on α and the oligosaccharides of β, we have not observed changes between sites on α (see Amler et al., 1992).

DISCUSSION

In this work the oligosaccharides of the β-subunit of lamb kidney Na^+,K^+-ATPase were labeled with the fluorophore lucifer yellow. The steady-state and dynamic fluorescence properties of the free and bound probe were used to investigate the environment in which the carbohydrates of β reside, to identify potential α-β interactions and to measure distances between the carbohydrates of β and different regions of the enzyme, including the cardiac glycoside and the ATP binding domains. Our work confirmed the original observations by Lee and Fortes (1985) that the LY labeling was specific for the oligosaccharides of β and the probe caused no change in enzyme activity or cardiac glycoside binding to the α-subunit. We further found no shift in the absorption, or fluorescence emission spectra of LY upon labeling, but its fluorescence intensity was quenched 10% by a static (lifetime-independent) process. The quenching of LY attached to solvent-exposed carbohydrate sites may be due to contact with amino acids in the protein or phospholipids in the membrane, because SDS denaturation of these structures relieved the quenching.

Fluorescence lifetime studies of enzyme-bound LY using frequency-domain fluorometry that have not been previously reported show that there may be significant heterogeneity in the microenvironments about the LY labeling sites. After binding to the enzyme the frequency-response curve was best fit by two lifetimes or a bimodal lifetime distribution, and free LY demonstrated a single discrete lifetime.

This heterogeneity was further defined using the carbohydrate-bound LY as an acceptor of nonradiative energy transfer from AO bound to the cardiac glycoside binding site. Steady-state measurements clearly demonstrated energy transfer, and dynamic lifetime measurements revealed a close proximity of the probes. According to the frequency domain results the distance distribution was centered at 18 Å, and an average distance calculated from steady-state intensity measurements was 34 Å. The 34 Å should be an overestimate due to the AO population that was unaffected by the presence of acceptors. This fraction represented only 10% of the lifetime distribution, but as a consequence of its relatively long lifetime it contributed 50% of the steady-state fluorescence intensity. We therefore propose that for our lamb enzyme preparation the majority of the LY molecules are considerably closer to AO than our initial steady-state 34 Å measurement or the 47 Å calculated by Lee and Fortes (1986) using the dog kidney enzyme, which has a somewhat more extended sugar arrangement for its glycans than does the lamb enzyme (Treuheit et al., 1993). The large 16 Å half-width of the distribution about the average distance (18 Å) then indicates the existence of more than one donor-acceptor distance (Lakowicz et al., 1988). The availability of 10–12 potential LY labeling sites per β-subunit (Lee and Fortes, 1985; Treuheit et al., 1993) but only a single AO binding site suggests the distribution of multiple LY acceptors about a single AO donor fluorophore.

The FET-determined distances from LY to AO and ErITC, and between AO and ErITC, were then used to model the LY position relative to the membrane surface. The three points can be thought of as forming a triangle, with LY 81–88 Å from ErITC and 18 Å from AO, and an ErITC-to-AO distance of 70 Å (Amler et al., 1992; Carilli et al., 1982). Fig. 5 represents these three site locations with their hypothetical positions somewhat localized by considering the information available. For example, using our previous FET measurements between ErITC and FITC bound at the ATP binding sites of adjacent α-subunits of $(\alpha\beta)_2$ dimers, we have placed the ErITC label near the center of the intracellularly exposed mass of α. Next, the cardiac glycoside-binding site faces the extracellular side, and at least a portion of it should lie near the membrane surface of the short H^1H2 extracellular loop (Price and Lingrel, 1988). Although its distance from the dimer center on the extracellular surface has not been estimated, its location is somewhat constrained, as Hebert et al. (1985, 1990) have determined from electron microscopy studies, which show that the extracellular side cross-sectional dimensions approximate a 60 Å × 30 Å oval. Fig. 5 therefore shows a model with the AO site located both directly above ErITC and with a lateral displacement of about 30 Å. If AO were to reside directly above the ErITC site, the average LY distance above the membrane could be ~18–14 Å, or less depending upon ligands present. Then if the AO shift is maximized, the LY sites again would be only about 18 Å or

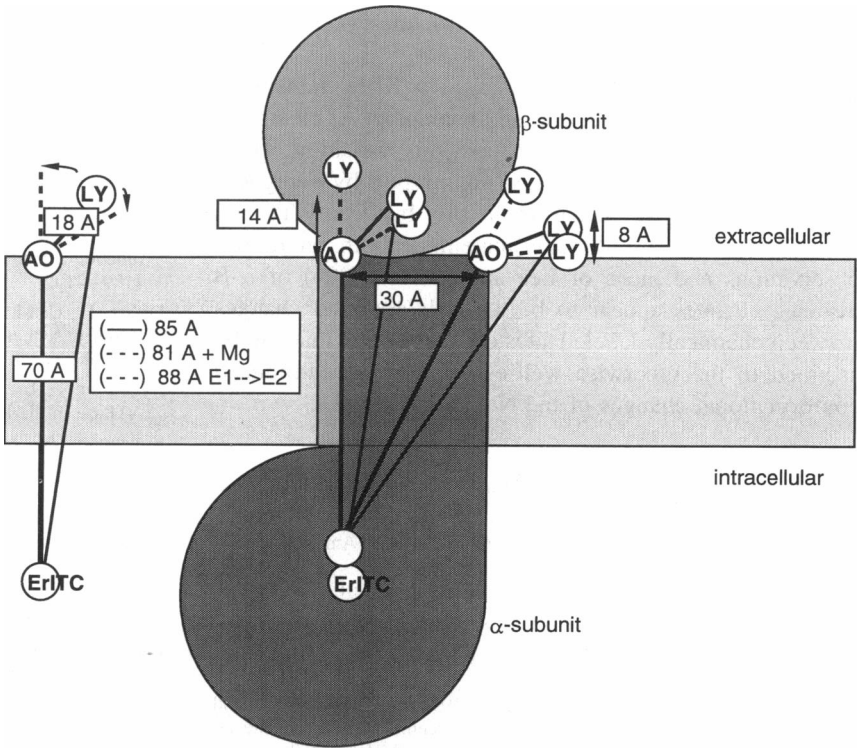

FIGURE 5 A model of the possible horizontal and vertical displacements of LY from AO at the membrane surface. In the simplest arrangement the labeling sites for AO and ErITC lie approximately on a straight line perpendicular to the plane of the membrane in the initial position shown in the figure, with ErITC lying 30 Å from the membrane and centered in the intracellular portion of the subunit and LY 18 Å from the AO site and approximately 81–88 Å from ErITC. The AO site could then be located 0–30 Å from a location directly above the ATP site. The uncertainty in the AO position includes a 26° angle of maximum tilt in the AO-ErITC line, and the placement of ErITC closer to the membrane. This also places the average LY locations 18 Å or less above the membrane, depending upon its lateral displacement from the AO binding site and the cations present.

less from the membrane surface. It would appear then that the LYs on the β-subunit carbohydrates are close to both the α-subunit and the membrane surface. This is quite different from the 36–45 Å distance from the membrane surface suggested by Lee and Fortes (1986), but their estimate was based only upon the AO-to-LY FET values, whereas this current estimate is also constrained by the LY-to-ErITC distance determination. The obvious major weaknesses in our model, however, are the somewhat ambiguous nature of the placement of ErITC in the center of the α-subunit, the heterogeneity in the carbohydrate locations, and the small FET values.

Further insight into the αβ subunit structure was derived from determining the effects of ligands upon LY fluorescence. Interestingly, no changes in spectral properties of LY were observed after the Na^+- and K^+-induced conformational transitions of the enzyme, but as observed by Lee and Fortes (1986) with the dog kidney enzyme, millimolar concentrations of divalent metal ions decreased the fluorescence of bound LY and caused a modest blueshift of its emission spectra, suggesting a change to a somewhat less polar environment. Mg^{2+} addition also reduced the heterogeneity of the LY fluorescence lifetimes, with most of the fluorescence intensity accounted for by a 4.4 ns lifetime component with a narrow (0.5 ns) half-width of distribution and decreased the ErITC-LY distance by approximately 4 Å.

The enzyme inhibitor oligomycin is known to alter the enzyme's responses to Na^+ and K^+ (Esmann, 1991; Plesner and Plesner, 1991); inhibiting the ligand caused $E_1 \rightarrow E_2$ and $E_1 \rightarrow E_2$-P enzyme conformational changes. We found that it affected the fluorescence of LY linked to the β-subunit and reduced the average AO-LY distance by about 2 Å. Our results suggest that it alters the structure of both α- and β-subunits.

Furthermore, although the $Na^+E_1 \Leftrightarrow K^+E_2$ transitions did not alter LY fluorescence, an apparent (3 Å) change in the ErITC-LY distance accompanied this transition. Thus, other than a recent, unelaborated upon report by Taniguchi and Mardh (1993) of changes in the FET between FITC and *N*-(*p*-(2-benzimidazolyl)phenyl)maleimide both on α, our observations and those of Lee and Fortes (1986) of α-β distance changes appear to be the only reported changes between chemically labeled sites on the enzyme that can be ascribed to the otherwise well-established ligand-induced conformational changes of the Na^+,K^+-ATPase.

This work was supported by National Health Institute research grant RO1-HL32214 (W. J. B.), a National American Heart Association grant-in-aid (W. J. B.), and a Southwestern Ohio Chapter American Heart Association Fellowship (A. A.).

REFERENCES

Abbott, A., E. Amler, and W. J. Ball, Jr. 1991. Immunochemical and spectroscopic characterization of two fluorescein 5′-isothiocyanate labeling sites on Na^+,K^+-ATPase. *Biochemistry.* 30:7155–7162.

Amler, E., A. Abbott, and W. J. Ball, Jr. 1992. Structural dynamics and oligomeric interactions of Na^+,K^+-ATPase as monitored using fluorescence energy transfer. *Biophys. J.* 61:553–568.

Arystarkhova, E., D. L. Gibbons, and K. J. Sweadner. 1995. Topology of the Na^+,K^+-ATPase. *J. Biol. Chem.* 270:8785–8796.

Brown, T. A., B. Horowitz, R. P. Miller, A. McDonough, and R. A. Farley. 1987. Molecular cloning and sequence analysis of the Na^+,K^+-ATPase β subunit from dog kidney. *Biochim. Biophys. Acta.* 912:244–253.

Carilli, C. T., R. A. Farley, D. M. Perlman, and L. C. Cantley. 1982. The active site structure of Na^+- and K^+-stimulated ATPase. *J. Biol. Chem.* 257:5601–5606.

Collins, J. H., and J. Leszyk. 1987. The "γ subunit" of Na^+,K^+-ATPase: a small, amphiphilic protein with a unique amino acid sequence. *Biochemistry.* 26:8665–8668.

Chow, D. C., and J. G. Forte. 1995. Functional significance of β subunit for heterodimeric P-type ATPases. *J. Exp. Biol.* 198:1–17.

Cornelius, F., and J. C. Skou. 1985. Na^+-Na^+ exchange mediated by Na^+,K^+-ATPase reconstituted into liposomes. *Biochim. Biophys. Acta.* 818:211–221.

Eakle, K. A., K. S. Kim, M. A. Kabalin, and R. A. Farley. 1992. High affinity ouabain binding by yeast cells expressing Na^+,K^+-ATPase α subunits and the gastric H^+,K^+-ATPase β subunit. *Proc. Natl. Acad. Sci. USA.* 89:2834–2838.

Eakle, K. A., R.-M. Lyu, and R. A. Farley. 1995. The influence of β-subunit on the interaction of Na^+,K^+-ATPase complexes with Na^+. *J. Biol. Chem.* 270:13937–13947.

Esmann, M. 1991. Oligomycin interaction with Na^+,K^+-ATPase: oligomycin binding and dissociation are slow processes. *Biochem. Biophys. Acta.* 1064:31–36.

Fiorini, R., M. Valentino, S. Wang, M. Glaser, and E. Gratton. 1987. Fluorescence lifetime distributions of 3,6-diphenyl 1,3,5-hexatriene in phospholipid vesicles. *Biochemistry.* 26:3864–3870.

Fortes, P. A. G. 1986. A fluorometric method for the determination of functional (Na^+-K^+)-ATPase and cardiac glycoside receptors. *Anal. Biochem.* 158:454–462.

Geering, K. 1991. Posttranslational modifications and intracellular transport of Na^+-pumps: importance of subunit assembly. *In* The Sodium Pump: Structure, Mechanism and Regulation. Rockefeller Press, New York. 31–43.

Geering, K., I. Theulaz, F. Verney, M. T. Haüptle, and B. C. Rossier. 1989. A role for the β-subunit in the expression of functional Na^+,K^+-ATPase in *Xenopus* oocytes. *Am. J. Physiol.* 257:C851–C858.

Hebert, H., E. Skriver, U. Kaveus, and A. B. Maunsbach. 1990. Coexistence of different forms of Na^+,K^+-ATPase in two-dimensional membrane crystals. *FEBS Lett.* 268:83–87.

Hebert, H., E. Skriver, and A. B. Maunsbach. 1985. Three dimensional structure of renal Na^+,K^+-ATPase determined by electron microscopy of membrane crystals. *FEBS Lett.* 187:182–186.

Horowitz, B., K. A. Eakle, G. Scheiner-Bobis, G. R. Randolph, C. Y. Chen, R. A. Hitzeman, and R. A. Farley. 1990. Synthesis and assembly of functional mammalian Na^+,K^+-ATPase in yeast. *J. Biol. Chem.* 265: 4189–4192.

Jaisser, F., C. M. Canessa, J.-D. Horisberger, and B. C. Rossier. 1992. Primary sequence and functional expression of a mouse ouabain-resistant Na^+,K^+-ATPase. *J. Biol. Chem.* 267:16895–16903.

Jorgensen, P. L. 1986. Structural, function and regulation of Na^+,K^+-ATPase in the kidney. *Kidney Int.* 29:10–20.

Kawamura, M., and K. Nagano. 1984. Evidence for essential disulfide bonds in the α subunit of Na^+,K^+-ATPase. *Biochim. Biophys. Acta.* 774:188–192.

Kirley, T. L. 1989. Determination of three disulfide bonds and one free sulfhydryl in the βsubunit of Na^+,K^+-ATPase. *J. Biol. Chem.* 264: 7185–7192.

Kirley, T. L. 1990. Inactivation of Na^+,K^+-ATPase by β-mercaptoethanol. *J. Biol. Chem.* 265:4227–4232.

Laczko, G., I. Gryczynski, Z. Gryczynski, W. Wiczk, H. Malak, and J. R. Lakowicz. 1990. A 10-GHz frequency-domain fluorometer. *Rev. Sci. Instrum.* 61:2331–2337.

Laemmli, U. K. 1970. Cleavage of structural proteins during the assembly of the head of bacteriophage T4. *Nature.* 227:680–685.

Lakowicz, J. R. 1983. Principles of Fluorescence Spectroscopy. Plenum Press, New York.

Lakowicz, J. R., E. Gratton, G. Laczko, H. Cherek, and M. Limkemann. 1984. Analysis of frequency decay kinetics from variable-frequency phase shift and modulation data. *Biophys. J.* 46:463–477.

Lakowicz, J. R., I. Gryczynski, H. C. Cheung, C. Wang, M. L. Johnson, and N. Joshi. 1988. Distance distributions in proteins recovered by frequency-domain fluorometry. *Biochemistry.* 27:9149–9160.

Lakowicz, J. R., G. Laczko, and I. Gryczynski. 1986. A 2-GHZ frequencydomain fluorometer. *Rev. Sci. Instrum.* 57:2499–2506.

Lakowicz, J. R., R. Jayaweera, N. Joshi, and I. Gryczynski. 1987a. Correction for contaminant fluorescence in frequency domain fluorometry. *Anal. Biochem.* 160:471–179.

Lakowicz, J. R., M. L. Johnson, W. Wiczk, A. Bhoat, and R. F. Steiner. 1987b. Resolution of a distribution of distance by fluorescence energy transfer and frequency-domain fluorometry. *Chem. Phys. Lett.* 138:587–593.

Lakowicz, J. R., J. Kusba, W. Wiczk, I. Grycsznski, and M. L. Johnson. 1990. End-to-end diffusion of flexible β-chromophore molecules observed by intramolecular energy transfer and frequency-domain fluorometry. *Chem. Phys. Lett.* 173:319–326.

Lane, L. K., J. D. Potter, and J. H. Collins. 1979. Large-scale purification of Na, K-ATPase and its protein subunits from lamb-kidney medulla. *Prep. Biochem.* 9:157–190.

Lee, J., and P. G. A. Fortes. 1985. Labeling of the glycoprotein subunit of (Na^+,K^+)ATPase with fluorescent probes. *Biochemistry.* 24:322–332.

Lee, J. A., and P. A. G. Fortes. 1986. Spatial relationship and conformational changes between the cardiac glycoside site and β-subunit oligosaccharides in sodium plus potassium activated adenosine triphosphate. *Biochemistry.* 25:8133–8141.

Lowry, O. H., N. J. Rosebrough, A. L. Farr, and R. J. Randall. 1951. Protein measurement with the Folin phenol reagent. *J. Biol. Chem.* 193:2165–2175.

Lutsenko, S., and J. H. Kaplan. 1993. An essential role for the extracellular domain of the Na^+,K^+-ATPase β-subunit in cation occlusion. *Biochemistry.* 32:6737–6743.

Noguchi, S., M. Mishina, E. M. Kawamura, and S. Numa. 1987. Expression of functional Na^+,K^+-ATPase from cloned cDNAs. *FEBS Lett.* 225:27–32.

Ohta, T., M. Yoshida, K. Nagano, H. Hirano, and M. Kawamura. 1986. Structure of the extra-membranous domain of the β subunit of Na^+,K^+-ATPase revealed by its tryptic peptides. *FEBS Lett.* 204:297–301.

Plesner, L., and I. W. Plesner. 1991. Kinetics of oligomycin inhibition and activation of Na^+,K^+-ATPase. *Biochim. Biophys. Acta.* 1076:421–426.

Price, E., and J. B. Lingrel. 1988. Structure-function relationships in the Na^+,K^+-ATPase subunit. *Biochemistry.* 27:8400–8408.

Schwartz, A., J. C. Allen, and S. J. Harigaya. 1969. Possible involvement of cardiac Na^+,K^+-adenosine triphosphatase in the mechanism of action of cardiac glycosides. *J. Pharmacol. Exp. Ther.* 168:31–41.

Shull, G. E., L. K. Lane, and J. B. Lingrel. 1986. Amino-acid sequence of the β-subunit of the Na^+,K^+-ATPase deduced from a cDNA. *Nature.* 321:429–431.

Stewart, W. W. 1978. Functional corrections between cells as revealed by dye-coupling with a highly fluorescent naphthalimide tracer. *Cell.* 14: 741–759.

Sun, Y., and W. J. Ball, Jr. 1994. Identification of antigenic sites on the Na^+,K^+-ATPase β-subunit. *Biochim. Biophys. Acta.* 1207:236–248.

Tamkun, M. M., and D. M. Fambrough. 1986. The Na^+,K^+-ATPase of chick sensory neurons. *J. Biol. Chem.* 261:1009–1019.

Taniguchi, K., and S. Mardh. 1993. Reversible changes in the fluorescence energy transfer accompanying formation of reaction intermediates in probe-labeled (Na^+,K^+)-ATPase. *J. Biol. Chem.* 268:15588–15594.

Taniguchi, K., T. Sasaki, E. Shinoguchi, Y. Kamo, and E. Ito. 1991. Conformational change accompanying formation of oligomycin-induced Na^+-bound forms and their conversion to ADP-sensitive phosphoenzymes in Na^+,K^+-ATPase. *J. Biochem.* 109:299–306.

Treuheit, M. J., C. E. Costello, and T. L. Kirley. 1993. Structures of the complex glycans found on the β-subunit of (Na,K)-ATPase. *J. Biol. Chem.* 268:13914–13919.

Zamofing, D., B. C. Rossier, and K. Geering. 1988. Role of the Na^+,K^+-ATPase β subunit in the cellular accumulation and maturation of the enzyme as assessed by glycosylation inhibitors. *J. Membr. Biol.* 104: 69–79.